Chapter 1

# Substructuring Method in Structural Health Monitoring

Shun Weng, Hong-Ping Zhu, Yong Xia and Fei Gao

Additional information is available at the end of the chapter

http://dx.doi.org/10.5772/67890

## Abstract

In sensitivity-based finite element model updating, the eigensolutions and eigensensitivities are calculated repeatedly, which is a time-consuming process for large-scale structures. In this chapter, a forward substructuring method and an inverse substructuring method are proposed to fulfill the model updating of large-scale structures. In the forward substructuring method, the analytical FE model of the global structure is divided into several independent substructures. The eigensolutions of each independent substructure are used to recover the eigensolutions and eigensensitivities of the global structure. Consequently, only some specific substructures are reanalyzed in model updating and assembled with other untouched substructures to recover the eigensolutions and eigensensitivities of the global structure. In the inverse substructuring method, the experimental modal data of the global structure are disassembled into substructural flexibility. Afterwards, each substructure is treated as an independent structure to reproduce its flexibility through a model-updating process. Employing the substructuring method, the model updating of a substructure can be conducted by measuring the local area of the concerned substructure solely. Finally, application of the proposed methods to a laboratory tested frame structure reveals that the forward and inverse substructuring methods are effective in model updating and damage identification.

**Keywords:** structural health monitoring, substructuring method, damage identification, eigensolutions, eigensensitivity

# 1. Introduction

Accurate finite element (FE) models are essential in damage identification and condition assessment for structural health monitoring. In vibration-based model-updating process, the FE model of a structure is iteratively updated to guarantee its vibration properties to reproduce the measured counterparts in an optimal manner [1]. In the optimization process, the structural responses are usually used to construct the objective function. The response sensitivities, which are the first derivatives of the structural responses to some structural physical parameters, are used to indicate a rapid searching direction. In this regard, the eigensolutions and their associated sensitivity matrices of the analytical model are required to be gained repeatedly in each iteration [2, 3]. The majority of the practical structures in civil engineering are large in scale, thus their FE models usually consists of a large number of degrees of freedom (DOFs) and uncertain updating parameters. The conventional model updating methods of large-scale structures are expensive in terms of computation time and computer memory [2].

It has been proved that the substructuring methods are efficient in dealing with large-scale structures, as it takes the local area as an independent structure [4–9]. First, the global structure is divided rationally into several smaller substructures to make it much easier and faster to analyze the small substructures independently. Second, the FE model of a substructure has much fewer uncertain parameters than the global structure, which helps to accelerate the convergence of optimization process to identify these parameters and alleviates the ill-condition problems. Third, the substructuring method is required to measure the local area of the practical structure and save the experimental instruments. Finally, the substructuring method can be more promising if combined with parallel computation.

In this chapter, a forward substructuring method and an inverse substructuring method are proposed for model updating and damage identification. In the forward substructuring method, the divided substructures are analyzed independently and are assembled to recover the eigensolutions of the global structure by satisfying the coordination condition of displacement at the interfaces. Afterwards, the fast-calculated eigensolutions and eigensensitivities of the global structure are used for model updating. In the inverse substructuring method, the experimental modal data of the global structure are disassembled into the substructural flexibility by satisfying the coordination condition of force and displacement at the interfaces. Based on the extracted substructural flexibility, the model-updating process is performed on the concerned substructure by treating it as an independent structure. In the following part, the forward and inverse substructuring methods will be explained first and then the two kinds of substructure-based model updating methods will be verified by a laboratory-tested frame structure.

# 2. Forward substructuring method

## 2.1. Eigensolutions

In the forward substructuring method, the eigensolutions and eigensensitivities of a substructure are calculated and assembled to recover those of the global structure. The global structure

is divided into $N_S$ independent substructures, and the number of DOFs of each substructure is $n_j$ ($j$ = 1,2,…, $N_S$). Treated as an independent structure, the eigenequation of the $j$th substructure is expressed as

$$\mathbf{K}^{(j)}\{\phi_i^{(j)}\} = \lambda_i^{(j)}\mathbf{M}^{(j)}\{\phi_i^{(j)}\} \tag{1}$$

where $\mathbf{K}(j)$ and $\mathbf{M}(j)$ are the stiffness matrix and mass matrix of the $j$th substructure, respectively. ($\phi i(j)$, $\lambda i(j)$) are the $i$th eigenpairs of the $j$th substructure. The $n^{(j)}$ pairs of eigenvalues and eigenvectors are expressed as [10]

$$\mathbf{\Lambda}^{(j)} = Diag\left[\lambda_1^{(j)}, \lambda_2^{(j)}, \ldots, \lambda_{n_j}^{(j)}\right], \mathbf{\Phi}^{(j)} = \left[\phi_1^{(j)}, \phi_2^{(j)}, \ldots, \phi_{n_j}^{(j)}\right],$$

And due to orthogonality, eigenvectors satisfy the two following formulas as

$$\left[\mathbf{\Phi}^{(j)}\right]^T\mathbf{K}^{(j)}\mathbf{\Phi}^{(j)} = \mathbf{\Lambda}^{(j)}, \left[\mathbf{\Phi}^{(j)}\right]^T\mathbf{M}^{(j)}\mathbf{\Phi}^{(j)} = n_j$$

The eigensolutions of the global structure can be recovered by adding constraints at the interfaces to obey the principle of virtual work and geometric compatibility like [11]

$$\begin{bmatrix} \mathbf{\Lambda}^p - \overline{\lambda}\mathbf{I} & -\mathbf{\Gamma} \\ -\mathbf{\Gamma}^T & \mathbf{0} \end{bmatrix}\begin{Bmatrix} \mathbf{z} \\ \tau \end{Bmatrix} = \begin{Bmatrix} \mathbf{0} \\ \mathbf{0} \end{Bmatrix} \tag{2}$$

where

$$\begin{aligned} &\mathbf{\Gamma} = [\mathbf{C}\mathbf{\Phi}^p]^T, \mathbf{\Lambda}^p = Diag\left[\mathbf{\Lambda}^{(1)}, \mathbf{\Lambda}^{(2)}, \ldots, \mathbf{\Lambda}^{(N_s)}\right] \\ &\mathbf{\Phi}^p = Diag\left[\mathbf{\Phi}^{(1)}, \mathbf{\Phi}^{(2)}, \ldots, \mathbf{\Phi}^{(N_s)}\right] \end{aligned} \tag{3}$$

Matrix **C** gives the general implicit constraints to guarantee the nodes at the interface identical displacement [11]. **C** contains two nonzero elements in each row, which are 1 and −1 for a rigid interface connection. $\mathbf{\Lambda}^p$ and $\mathbf{\Phi}^p$ are diagonally assembled from the eigensolutions of each substructure. $\overline{\lambda}$ is the eigenvalue of the global structure, which is the square of circular frequencies. The eigenvectors of the global structure are recovered by $\overline{\mathbf{\Phi}} = \mathbf{\Phi}^p\{\mathbf{z}\}$. τ indicates the interface forces between the adjacent substructures. Superscript "$p$" denotes the primitive matrices, which is assembled diagonally from the substructural matrices before displacement constraints at the adjacent substructures are imposed.

It is noted from Eq. (2) that $\mathbf{\Lambda}^p$ and $\mathbf{\Phi}^p$ are assembled from all modes of the substructures. It is inefficient and unworthy with all eigenmodes available, as only the first few eigenmodes are usually required for a large-scale structure. Here, the first few eigensolutions of each substructure are selected as "master" modes, and the residual higher modes are the "slave" modes. Only the master modes are used to gain the eigenequation of the global structure.

From here on, subscript "$m$" represents the "master" modes and subscript "$s$" denotes the "slave" modes, respectively. The eigenequation (Eq. (2)) is then rewritten according to the master modes and slave modes as

$$\begin{bmatrix} \mathbf{\Lambda}_m^p - \overline{\lambda}\mathbf{I} & \mathbf{0} & -\mathbf{\Gamma}_m \\ \mathbf{0} & \mathbf{\Lambda}_s^p - \overline{\lambda}\mathbf{I} & -\mathbf{\Gamma}_s \\ -\mathbf{\Gamma}_m^T & -\mathbf{\Gamma}_s^T & \mathbf{0} \end{bmatrix} \begin{Bmatrix} \mathbf{z}_m \\ \mathbf{z}_s \\ \tau \end{Bmatrix} = \begin{Bmatrix} \mathbf{0} \\ \mathbf{0} \\ \mathbf{0} \end{Bmatrix} \tag{4}$$

where

$$\begin{aligned} &\mathbf{\Lambda}_m^p = Diag[\mathbf{\Lambda}_m^{(1)}, \mathbf{\Lambda}_m^{(2)}, \ldots, \mathbf{\Lambda}_m^{(j)}, \ldots, \mathbf{\Lambda}_m^{(N_s)}], \mathbf{\Lambda}_m^{(j)} = Diag[\lambda_1^{(j)}, \lambda_2^{(j)}, \ldots, \lambda_{m^{(j)}}^{(j)}] \\ &\mathbf{\Phi}_m^p = Diag[\mathbf{\Phi}_m^{(1)}, \mathbf{\Phi}_m^{(2)}, \ldots, \mathbf{\Phi}_m^{(j)}, \ldots, \mathbf{\Phi}_m^{(N_s)}], \mathbf{\Phi}_m^{(j)} = [\phi_1^{(j)}, \phi_2^{(j)}, \ldots, \phi_{m^{(j)}}^{(j)}] \\ &\mathbf{\Lambda}_s^p = Diag[\mathbf{\Lambda}_s^{(1)}, \mathbf{\Lambda}_s^{(2)}, \ldots, \mathbf{\Lambda}_s^{(j)}, \ldots, \mathbf{\Lambda}_s^{(N_s)}], \mathbf{\Lambda}_s^{(j)} = Diag[\lambda_{m^{(j)}+1}^{(j)}, \lambda_{m^{(j)}+2}^{(j)}, \ldots, \lambda_{m^{(j)}+s^{(j)}}^{(j)}] \\ &\mathbf{\Phi}_s^p = Diag[\mathbf{\Phi}_s^{(1)}, \mathbf{\Phi}_s^{(2)}, \ldots, \mathbf{\Phi}_s^{(j)}, \ldots, \mathbf{\Phi}_s^{(N_s)}], \mathbf{\Phi}_s^{(j)} = [\phi_{m^{(j)}+1}^{(j)}, \phi_{m^{(j)}+2}^{(j)}, \ldots, \phi_{m^{(j)}+s^{(j)}}^{(j)}] \\ &\mathbf{\Gamma}_m = [\mathbf{C}\mathbf{\Phi}_m^p]^T, \mathbf{\Gamma}_s = [\mathbf{C}\mathbf{\Phi}_s^p]^T \\ &m^p = \sum_{j=1}^{N_s} m_j, s^p = \sum_{j=1}^{N_s} s_j, m_j + s_j = n_j (j = 1, 2, \ldots, N_s) \end{aligned} \tag{5}$$

According to the second line of Eq. (4), the slave coordinates can be expressed as

$$\mathbf{z}_s = (\mathbf{\Lambda}_s^p - \overline{\lambda})^{-1}\mathbf{\Gamma}_s\tau \tag{6}$$

Substitution of Eq. (6) into Eq. (4) gives

$$\begin{bmatrix} \mathbf{\Lambda}_m^p - \overline{\lambda}\mathbf{I} & -\mathbf{\Gamma}_m \\ -\mathbf{\Gamma}_m^T & -\mathbf{\Gamma}_s^T(\mathbf{\Lambda}_s^p - \overline{\lambda}\mathbf{I})^{-1}\mathbf{\Gamma}_s \end{bmatrix} \begin{Bmatrix} \mathbf{z}_m \\ \tau \end{Bmatrix} = \begin{Bmatrix} \mathbf{0} \\ \mathbf{0} \end{Bmatrix} \tag{7}$$

Generally, the lower eigenmodes are usually required by a structure. The eigenvalues $\overline{\lambda}$ are much smaller than $\mathbf{\Lambda}_s^p$ when the size of the master modes is selected rationally. In this regard, Eq. (7) is approximated as:

$$\begin{bmatrix} \mathbf{\Lambda}_m^p - \overline{\lambda}\mathbf{I} & -\mathbf{\Gamma}_m \\ -\mathbf{\Gamma}_m^T & -\mathbf{\Gamma}_s^T(\mathbf{\Lambda}_s^p)^{-1}\mathbf{\Gamma}_s \end{bmatrix} \begin{Bmatrix} \mathbf{z}_m \\ \tau \end{Bmatrix} = \begin{Bmatrix} \mathbf{0} \\ \mathbf{0} \end{Bmatrix} \tag{8}$$

The above eigenequation can be simplified by denoting $\tau$ with $\mathbf{z}_m$ from the second line of Eq. (8) and substituting it into the first line as:

$$[(\mathbf{\Lambda}_m^p - \overline{\lambda}\mathbf{I}_m) + \mathbf{\Gamma}_m\zeta^{-1}\mathbf{\Gamma}_m^T]\mathbf{z}_m = \mathbf{0} \tag{9}$$

Consequently, $\overline{\lambda}$ and $\mathbf{z}_m$ are available by solving Eq. (9) with commonly used eigensolver such as Simpson method or Lanczos method [10]. And the eigenvector of the global structure is recovered from the master modes by $\overline{\mathbf{\Phi}} = \mathbf{\Phi}_m^p\mathbf{z}_m$. The size of the simplified eigenequation (Eq. (9)) is equal to the number of the master modes, which is much smaller than the original one (Eq. (2)). It is noted from Eq. (9) that only the master eigensolutions of the independent substructures are used to gain the eigensolutions of the global structure. The contribution of the slave modes is compensated by the first-order residual flexibility $\zeta = \mathbf{\Gamma}_s^T(\mathbf{\Lambda}_s^p)^{-1}\mathbf{\Gamma}_s$, which is calculated by the master modes as:

$$\boldsymbol{\Gamma}_s^T(\boldsymbol{\Lambda}_s^p)^{-1}\boldsymbol{\Gamma}_s = \mathbf{C}\boldsymbol{\Phi}_s^p(\boldsymbol{\Lambda}_s^p)^{-1}[\boldsymbol{\Phi}_s^p]^T\mathbf{C}^T \tag{10}$$

$$\boldsymbol{\Phi}_s^p(\boldsymbol{\Lambda}_s^p)^{-1}[\boldsymbol{\Phi}_s^p]^T = \begin{bmatrix} \left(\mathbf{K}^{(1)}\right)^{-1} - \boldsymbol{\Phi}_m^{(1)}\left(\boldsymbol{\Lambda}_m^{(1)}\right)^{-1}[\boldsymbol{\Phi}_m^{(1)}]^T & & \\ & \ddots & \\ & & \left(\mathbf{K}^{(N_s)}\right)^{-1} - \boldsymbol{\Phi}_m^{(N_s)}\left(\boldsymbol{\Lambda}_m^{(N_s)}\right)^{-1}[\boldsymbol{\Phi}_m^{(N_s)}]^T \end{bmatrix}$$

### 2.2. Eigensensitivity

In this section, the eigensensitivity of the $i$th ($i$=1, 2, …, $N$) mode with respect to an elemental parameter will be derived. The elemental stiffness parameter $\alpha$ in the $A$th substructure is illustrated in the following. Writing Eq. (9) for the $i$th mode and differentiating it with respect to parameter $\alpha$ gives [11]

$$[(\boldsymbol{\Lambda}_m^p - \overline{\lambda}_i\mathbf{I}_m) + \boldsymbol{\Gamma}_m\zeta^{-1}\boldsymbol{\Gamma}_m^T]\frac{\partial\{\mathbf{z}_i\}}{\partial\alpha} + \frac{\partial[(\boldsymbol{\Lambda}_m^p - \overline{\lambda}_i\mathbf{I}_m) + \boldsymbol{\Gamma}_m\zeta^{-1}\boldsymbol{\Gamma}_m^T]}{\partial\alpha}\{\mathbf{z}_i\} = \{\mathbf{0}\} \tag{11}$$

Premultiplying $\{\mathbf{z}_i\}^T$ on both sides of Eq. (11) gives

$$\{\mathbf{z}_i\}^T[\boldsymbol{\Lambda}_m^p + \boldsymbol{\Gamma}_m\zeta^{-1}\boldsymbol{\Gamma}_m^T - \overline{\lambda}_i\mathbf{I}]\left\{\frac{\partial\mathbf{z}_i}{\partial\alpha}\right\} + \{\mathbf{z}_i\}^T\frac{\partial[\boldsymbol{\Lambda}_m^p + \boldsymbol{\Gamma}_m\zeta^{-1}\boldsymbol{\Gamma}_m^T - \overline{\lambda}_i\mathbf{I}]}{\partial\alpha}\{\mathbf{z}_i\} = 0 \tag{12}$$

Since $[(\boldsymbol{\Lambda}_m^p - \overline{\lambda}\mathbf{I}_m) + \boldsymbol{\Gamma}_m\zeta^{-1}\boldsymbol{\Gamma}_m^T]\mathbf{z}_m = \mathbf{0}$ (Eq. (9)) and $[\boldsymbol{\Lambda}_m^p + \boldsymbol{\Gamma}_m\zeta^{-1}\boldsymbol{\Gamma}_m^T - \overline{\lambda}_i\mathbf{I}]$ are a symmetric matrix, the first item on the left side of Eq. (12) is zero. In consequence, the $i$th eigenvalue derivative with respect to the designed parameter $\alpha$ is available by [12]

$$\frac{\partial\overline{\lambda}_i}{\partial\alpha} = \{\mathbf{z}_i\}^T\left[\frac{\partial\boldsymbol{\Lambda}_m^p}{\partial\alpha} + \frac{\partial(\boldsymbol{\Gamma}_m\zeta^{-1}\boldsymbol{\Gamma}_m^T)}{\partial\alpha}\right]\{\mathbf{z}_i\} \tag{13}$$

where

$$\frac{\partial(\boldsymbol{\Gamma}_m\zeta^{-1}\boldsymbol{\Gamma}_m^T)}{\partial\alpha} = \frac{\partial\boldsymbol{\Gamma}_m}{\partial\alpha}\zeta^{-1}\boldsymbol{\Gamma}_m^T - \boldsymbol{\Gamma}_m\zeta^{-1}\frac{\partial\zeta}{\partial\alpha}\zeta^{-1}\boldsymbol{\Gamma}_m^T + \boldsymbol{\Gamma}_m\zeta^{-1}\frac{\partial\boldsymbol{\Gamma}_m^T}{\partial\alpha} \tag{14}$$

$\frac{\partial\boldsymbol{\Lambda}_m^p}{\partial\alpha}$ and $\frac{\partial\boldsymbol{\Gamma}_m}{\partial\alpha}$ are the eigenvalue and eigenvector derivatives of the master modes of the independent substructures, respectively. $\frac{\partial\zeta}{\partial\alpha} = \frac{\partial\left(\boldsymbol{\Gamma}_s^T(\boldsymbol{\Lambda}_s^p)^{-1}\boldsymbol{\Gamma}_s\right)}{\partial\alpha}$ is the derivative of the residual flexibility of the substructures. Considering that the substructures are taken as independent structures, these derivative matrices are calculated within the $A$th substructure solely, while the corresponding derivative matrices in other substructures are zero matrices, i.e.,

$$\begin{aligned} &\frac{\partial\boldsymbol{\Lambda}_m^p}{\partial\alpha} = \begin{bmatrix} \mathbf{0} & \mathbf{0} & \mathbf{0} \\ \mathbf{0} & \frac{\partial\boldsymbol{\Lambda}_m^{(A)}}{\partial\alpha} & \mathbf{0} \\ \mathbf{0} & \mathbf{0} & \mathbf{0} \end{bmatrix}, \frac{\partial\boldsymbol{\Gamma}_m^T}{\partial\alpha} = \mathbf{C}\frac{\partial\boldsymbol{\Phi}_m^p}{\partial\alpha} = \mathbf{C}\begin{bmatrix} \mathbf{0} & \mathbf{0} & \mathbf{0} \\ \mathbf{0} & \frac{\partial\boldsymbol{\Phi}_m^{(A)}}{\partial\alpha} & \mathbf{0} \\ \mathbf{0} & \mathbf{0} & \mathbf{0} \end{bmatrix} \\ &\frac{\partial\zeta}{\partial\alpha} = \frac{\partial\left[\left(\boldsymbol{\Gamma}_s^T(\boldsymbol{\Lambda}_s^p)^{-1}\boldsymbol{\Gamma}_s\right)^{-1}\right]}{\partial\alpha} = \mathbf{C}\begin{bmatrix} \mathbf{0} & \mathbf{0} & \\ \mathbf{0} & \frac{\partial\left(\left(\mathbf{K}^{(A)}\right)^{-1} - \boldsymbol{\Phi}_m^{(A)}\left(\boldsymbol{\Lambda}_m^{(A)}\right)^{-1}[\boldsymbol{\Phi}_m^{(A)}]^T\right)}{\partial\alpha} & \mathbf{0} \\ \mathbf{0} & \mathbf{0} & \mathbf{0} \end{bmatrix}\mathbf{C}^T \end{aligned} \tag{15}$$

$\frac{\partial \mathbf{\Lambda}_m^{(A)}}{\partial \alpha}$ and $\frac{\partial \mathbf{\Phi}_m^{(A)}}{\partial \alpha}$ can be calculated rapidly by treating the $A$th substructure as an independent structure with Nelson's method [12, 13].

The $i$th eigenvector of the global structure is recovered by the master modes as

$$\overline{\mathbf{\Phi}}_i = \mathbf{\Phi}_m^p \{\mathbf{z}_i\} \tag{16}$$

Eq. (16) is differentiated with respect to the structural parameter $\alpha$ as

$$\frac{\partial \overline{\mathbf{\Phi}}_i}{\partial \alpha} = \frac{\partial \mathbf{\Phi}_m^p}{\partial \alpha} \{\mathbf{z}_i\} + \mathbf{\Phi}_m^p \left\{\frac{\partial \mathbf{z}_i}{\partial \alpha}\right\} \tag{17}$$

where $\mathbf{\Phi}_m^p$ and $\frac{\partial \mathbf{\Phi}_m^p}{\partial \alpha}$ are the master eigenvectors and their derivatives of the $A$th substructure, respectively. $\{\mathbf{z}_i\}$ is the eigenvector calculated from Eq. (9). Only $\left\{\frac{\partial \mathbf{z}_i}{\partial \alpha}\right\}$ is required to calculate the eigenvector derivative of the $i$th mode in Eq. (17).

$\left\{\frac{\partial \mathbf{z}_i}{\partial \alpha}\right\}$ is rewritten by the sum of a particular part and a general part as

$$\left\{\frac{\partial \mathbf{z}_i}{\partial \alpha}\right\} = \{v_i\} + c_i\{\mathbf{z}_i\} \tag{18}$$

where $c_i$ is a participation factor and $\{v_i\}$ is a residual vector. Substituting Eq. (18) into Eq. (11) leads to

$$[\mathbf{\Lambda}_m^p + \mathbf{\Gamma}_m \zeta^{-1} \mathbf{\Gamma}_m^T - \overline{\lambda}_i \mathbf{I}](\{v_i\} + c_i\{\mathbf{z}_i\}) = -\frac{\partial[\mathbf{\Lambda}_m^p + \mathbf{\Gamma}_m \zeta^{-1} \mathbf{\Gamma}_m^T - \overline{\lambda}_i \mathbf{I}]}{\partial r}\{\mathbf{z}_i\} \tag{19}$$

Given that $[\mathbf{\Lambda}_m^p + \mathbf{\Gamma}_m \zeta^{-1} \mathbf{\Gamma}_m^T - \overline{\lambda}_i \mathbf{I}]\{\mathbf{z}_i\} = \{\mathbf{0}\}$, Eq. (19) can be simplified into

$$\mathbf{\Psi}\{v_i\} = \{Y_i\} \tag{20}$$

where

$$\mathbf{\Psi} = [\mathbf{\Lambda}_m^p + \mathbf{\Gamma}_m \zeta^{-1} \mathbf{\Gamma}_m^T - \overline{\lambda}_i \mathbf{I}], \{Y_i\} = -\frac{\partial[\mathbf{\Lambda}_m^p + \mathbf{\Gamma}_m \zeta^{-1} \mathbf{\Gamma}_m^T - \overline{\lambda}_i \mathbf{I}]}{\partial \alpha}\{\mathbf{z}_i\} \tag{21}$$

In consequence, $\mathbf{\Psi}$ and $\{Y_i\}$ can be calculated from Eq. (21) since all of their items have been available in the calculation of the eigenvalue derivatives proposed in the former section.

If no repeated roots exist in Eq. (20), $\mathbf{\Psi}$ takes the size of $m^p \times m^p$ with the rank of ($m^p$-1). To solve this rank-deficient equation (Eq. (20)), the $k$th item (corresponds to the maximum entry in $\{\mathbf{z}_i\}$) in $\{v_i\}$ is assumed to be zero, and the corresponding row and column in $\mathbf{\Psi}$ and corresponding item in $\{Y_i\}$ are assumed to be zeros as well [14]. The full rank equation is formed as

$$\begin{bmatrix} \mathbf{\Psi}_{11} & \mathbf{0} & \mathbf{\Psi}_{13} \\ \mathbf{0} & 1 & \mathbf{0} \\ \mathbf{\Psi}_{31} & \mathbf{0} & \mathbf{\Psi}_{33} \end{bmatrix} \begin{Bmatrix} v_{i1} \\ v_{ik} \\ v_{i3} \end{Bmatrix} = \begin{Bmatrix} Y_{i1} \\ 0 \\ Y_{i3} \end{Bmatrix} \tag{22}$$

In consequence, the vector $\{v_i\}$ is solved from Eq. (22).

The eigenvectors $\{\mathbf{z}_i\}$ satisfy the orthogonal condition of

$$\{\mathbf{z}_i\}^T \{\mathbf{z}_i\} = 1 \tag{23}$$

Equation (23) is differentiated with respect to $\alpha$ as

$$\frac{\partial \{\mathbf{z}_i\}^T}{\partial \alpha} \{\mathbf{z}_i\} + \{\mathbf{z}_i\}^T \frac{\partial \{\mathbf{z}_i\}}{\partial \alpha} = 0 \tag{24}$$

Substitution of Eq. (18) into Eq. (24) gives

$$(\{v_i\}^T + c_i \{\mathbf{z}_i\}^T)\{\mathbf{z}_i\} + \{\mathbf{z}_i\}^T (\{v_i\} + c_i \{\mathbf{z}_i\}) = 0 \tag{25}$$

The participation factor $c_i$ is thus obtained as

$$c_i = -\frac{1}{2} (\{v_i\}^T \{\mathbf{z}_i\} + \{\mathbf{z}_i\}^T \{v_i\}) \tag{26}$$

Finally, the first-order derivative of $\{\mathbf{z}_i\}$ with respect to $\alpha$ is calculated by

$$\left\{\frac{\partial \mathbf{z}_i}{\partial \alpha}\right\} = \{v_i\} - \frac{1}{2} (\{v_i\}^T \{\mathbf{z}_i\} + \{\mathbf{z}_i\}^T \{v_i\}) \{\mathbf{z}_i\} \tag{27}$$

It is noted from Eq. (17) that the eigenvector derivatives of the global structure are calculated from $\mathbf{\Phi}_m^p$ and $\frac{\partial \mathbf{\Phi}_m^p}{\partial \alpha}$. $\left\{\frac{\partial \mathbf{z}_i}{\partial \alpha}\right\}$ and $\{\mathbf{z}\}$ are treated as the weights and are computed from the small-size eigenequation (Eq.(9)) rapidly. Only the derivative matrices of the master modes in the $A$th substructure are needed to recover the eigensensitivity of the global structure. As the size of the independent substructures is much smaller than that of the global structure, the proposed substructuring method can significantly improve the computational efficiency.

### 2.3. Substructure-based updating method

Based on the eigensolutions and eigensensitivities calculated with the forward substructuring method, the substructure-based model updating is described in **Figure 1** with an iterative process. In each iteration, the eigensolutions are calculated from the modified substructures with the above substructuring method and are then compared with the experimental modal data (frequencies and mode shapes) to construct the objective function. The substructure-based eigensensitivities with respect to a specific parameter are calculated from the substructure containing the concerned parameter, to indicate the searching direction in each optimal

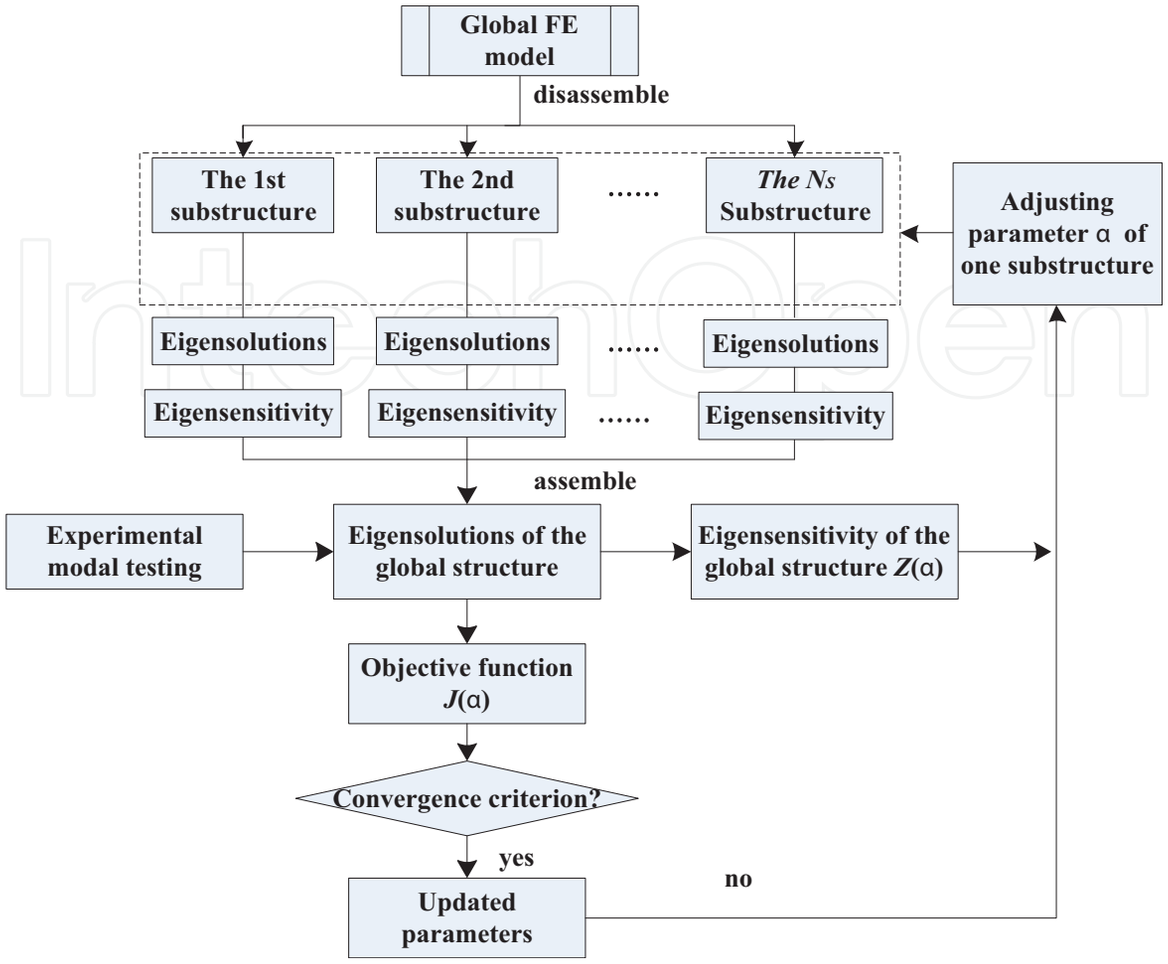


**Figure 1.** The model updating of forward substructuring method.

step. The objective function is minimized by adjusting the elemental parameters $\alpha$ iteratively according to the eigensensitivity matrices.

The objective function formed by the modal frequency and the mode shape is written as [14]

$$J(\alpha) = \sum_i W_{\lambda i}^2 \left[\lambda_i(\{\alpha\})^{FE} - {\lambda_i}^E\right]^2 + \sum_i W_{\phi i}^2 \sum_j \left[\phi_{ji}(\{\alpha\})^{FE} - {\phi_{ji}}^E\right]^2 \tag{28}$$

where ${\lambda_i}^E$ and ${\phi_{ji}}^E$ represent the experimental frequencies and mode shapes, respectively. ${\lambda_i}^{FE}$ and ${\phi_{ji}}^{FE}$ are the frequencies and mode shapes gained from the analytical FE model with the substructuring method (Eq.(8)) proposed above. $W_{\lambda i}$ and $W_{\phi i}$ are the weighting matrix of frequencies and mode shapes. The objective function is minimized by adjusting the elemental parameters $\alpha$ in an optimal manner.

The eigensensitivity is computed with the first derivative of a structural response with respect to a physical parameter as [2]

$$[S_\lambda(\alpha)] = \frac{\partial \lambda(\alpha)}{\partial \alpha}, [S_\phi(\alpha)] = \frac{\partial \phi(\alpha)}{\partial \alpha} \tag{29}$$

In this chapter, the eigensensitivity matrices are available with the forward substructuring method. They are computed solely from the derivative matrices of the substructure containing the concerned element, while the corresponding derivative matrices of all other substructures are zeros. As the calculation of eigensensitivity usually consumes most of the computation time when numerous elemental parameters are updated in practical model updating process, the forward substructuring method can significantly improve the computational efficiency of the model-updating process.

## 3. Inverse substructuring method

### 3.1. The extraction of substructural flexibility

In the inverse substructuring method, the global flexibility matrix estimated from the experimental modal data is disassembled into substructural flexibility matrices. Afterwards, the analytical FE models of the substructures are updated independently and parallelly to reproduce the extracted substructural flexibility matrices. As before, the global structure with $N$ DOFs is divided into $Ns$ independent substructures with the $j$th ($j = 1, 2, \ldots, Ns$) substructure $n^{(j)}$ DOFs. Treated as independent substructures, the substructural displacements, forces, stiffness, flexibility, and rigid body modes matrices are written in the primitive form as

$$\begin{aligned} &\{x^p\} = \left\{x^{(1)} \cdots x^{(j)} \cdots x^{(N_s)}\right\}^T, \{f^p\} = \left\{f^{(1)} \cdots f^{(j)} \cdots f^{(N_s)}\right\}^T \\ &\mathbf{K}^p = Diag\left[\mathbf{K}^{(1)} \cdots \mathbf{K}^{(j)} \cdots \mathbf{K}^{(N_s)}\right], \mathbf{F}^p = Diag\left[\mathbf{F}^{(1)} \cdots \mathbf{F}^{(j)} \cdots \mathbf{F}^{(N_s)}\right], \mathbf{R}^p = Diag\left[\mathbf{R}^{(1)} \cdots \mathbf{R}^{(j)} \cdots \mathbf{R}^{(N_s)}\right] \end{aligned} \tag{30}$$

where $\mathbf{K}^{(j)}$, $\mathbf{F}^{(j)}$, $x^{(j)}$, $f^{(j)}$, and $\mathbf{R}^{(j)}$, respectively, represent the stiffness, flexibility, nodal displacements, external forces, and rigid body modes of the $j$th substructure. It is noted that the rigid body modes $\mathbf{R}$ is related to free-constraint substructures. R is a zero matrix if the $j$th substructure is constrained after partition. Otherwise, $\mathbf{R}$ is determined by the nodal location. For example, a two-dimensional structure with $n$ nodes has three rigid body modes, i.e., the $x$ translation ($\mathbf{R}_x = 1$, $\mathbf{R}_y = 0$), the $y$ translation ($\mathbf{R}_x = 0$, $\mathbf{R}_y = 1$) and the $z$ rotation ($\mathbf{R}_x = -y$, $\mathbf{R}_y = x$), $\mathbf{R}$ takes the form of

$$\mathbf{R}^T = \begin{bmatrix} 1 & 0 & 0 & 1 & \cdots & 0 & 0 \\ 0 & 1 & 0 & 0 & \cdots & 1 & 0 \\ -y_1 & x_1 & 1 & -y_2 & \cdots & x_n & 1 \end{bmatrix} \tag{31}$$

The primitive forms of the substructural displacements and forces are associated with the global counterparts as [15]

$$\{x^p\} = \mathbf{L}^p\{x_g\}, [\mathbf{L}^p]^T\{f^p\} = \{f_g\} \tag{32}$$

where $\{x_g\}$ and $\{f_g\}$ are the nodal displacement and external force vector of the global structure. $\mathbf{L}^p$ is a Boolean matrix composed of 1 and 0 values to relate the DOFs of the substructures and the global structure [5]. Most of the values in $\mathbf{L}^p$ are zeros. $\mathbf{L}^p_{ij} = 1$ means that the $j$th DOF of the global structure corresponds to the $i$th DOF in the partitioned substructures. The displacement of an independent substructure is constituted by its deformational motions and rigid body motion

$$\{x^p\} = \mathbf{F}^p\{f^p\} + \mathbf{R}^p\{\beta^p\} \tag{33}$$

where $\beta$ is the participation factor of rigid body modes. As an independent structure, a substructure is excited by the external force and the internal interface force from the adjacent substructures as

$$\{f^p\} = ([\mathbf{L}^p]^T)^+\{f_g\} + \mathbf{C}\{\tau\} = \{\tilde{f}_g\} + \mathbf{C}\{\tau\} \tag{34}$$

where $\{\tilde{f}_g\} = ([\mathbf{L}^p]^T)^+\{f_g\} = \tilde{\mathbf{L}}^p\{f_g\}$, $\tilde{\mathbf{L}}^p = ([\mathbf{L}^p]^T)^+$is the generalized inverse of $[\mathbf{L}^p]^T$. Similar to the forward substructuring method, $\{\tau\}$ denotes the internal interface forces from the adjacent substructures, and matrix $\mathbf{C}$ implicitly defines the connections between the adjacent substructures. Substitution of Eq. (34) into Eq. (33) gives

$$\{x^p\} = \mathbf{F}^p(\{\tilde{f}_g\} + \mathbf{C}\{\tau\}) + \mathbf{R}^p\{\beta^p\} \tag{35}$$

Substitution of Eq. (35) into the left equation of Eq. (32) gives

$$\{x_g\} = [\mathbf{L}^p]^+\{x^p\} = [\tilde{\mathbf{L}}^p]^T\mathbf{F}^p(\{\tilde{f}_g\} + \mathbf{C}\{\tau\}) + [\tilde{\mathbf{L}}^p]^T\mathbf{R}^p\{\beta^p\} \tag{36}$$

Since the global displacement is associated with the global force by $\{x_g\} = \mathbf{F}_g\{f_g\}$ [15], the global flexibility can also be expressed as

$$\{x_g\} = [\mathbf{L}^p]^+\{x^p\} = [\tilde{\mathbf{L}}^p]^T\mathbf{F}^p(\{\tilde{f}_g\} + \mathbf{C}\{\tau\}) + [\tilde{\mathbf{L}}^p]^T\mathbf{R}^p\{\beta^p\} = \mathbf{F}_g\{f_g\} \tag{37}$$

Equation (37) means that the primitive substructural flexibility matrix $\mathbf{F}^p$ can be calculated from the global flexibility matrix $\mathbf{F}_g$ once the two variables $\{\tau\}$ and $\{\beta^p\}$ are given. $\{\tau\}$ and $\{\beta^p\}$ are gained according the force and displacement compatibility condition with the following procedures:

**1.** The primitive substructural rigid body modes and forces satisfy the force equilibrium compatibility as [16, 17]>

$$[\mathbf{R}^p]^T\{f^p\} = \{\mathbf{0}\} \tag{38}$$

**2.** From the physical point of view, matrix $\mathbf{C}$ constraints the displacement compatibility as

$$\mathbf{C}^T\{x^p\} = \{\mathbf{0}\} \tag{39}$$

http://dx.doi.org/10.5772/67890

Substituting Eqs. (33) and (34) into Eq. (39) leads to

$$\mathbf{C}^T\{\mathbf{F}^p(\{\tilde{f}_g\}+\mathbf{C}\{\tau\})+\mathbf{R}^p\{\beta^p\}\}=\{\mathbf{0}\} \tag{40}$$

Therefore, $\{\tau\}$ is expressed as

$$\{\tau\}=-\mathbf{F}_C^{-1}(\mathbf{C}^T\mathbf{F}^p\{\tilde{f}_g\}+\mathbf{R}_C\{\beta^p\}) \tag{41}$$

where $\mathbf{F}_C=\mathbf{C}^T\mathbf{F}^p\mathbf{C}$ and $\mathbf{R}_C=\mathbf{C}^T\mathbf{R}^p$.

The combination of Eq. (34) and Eq. (41) gives

$$[\mathbf{R}^p]^T\left(\{\tilde{f}_g\}-\mathbf{C}\mathbf{F}_C^{-1}(\mathbf{C}^T\mathbf{F}^p\{\tilde{f}_g\}+\mathbf{R}_C\{\beta^p\})\right)=\{\mathbf{0}\} \tag{42}$$

$\{\beta^p\}$ is therefore solved as

$$\{\beta^p\}=\mathbf{K}_R^{-1}([\mathbf{R}^p]^T-\mathbf{R}_C^T\mathbf{F}_C^{-1}\mathbf{C}^T\mathbf{F}^p)\{\tilde{f}_g\} \tag{43}$$

where $\mathbf{K}_R=\mathbf{R}_C^T\mathbf{F}_C^{-1}\mathbf{R}_C$. In consequence, $\{\tau\}$ is therefore solved from Eq. (41) as

$$\{\tau\}=-\mathbf{F}_C^{-1}\mathbf{C}^T\mathbf{F}^p\{\tilde{f}_g\}+\mathbf{F}_C^{-1}\mathbf{C}^T\mathbf{R}^p\mathbf{K}_R^{-1}([\mathbf{R}^p]^T\mathbf{K}_C\mathbf{F}^p-[\mathbf{R}^p]^T)\{\tilde{f}_g\} \tag{44}$$

where $\mathbf{K}_C=\mathbf{C}\mathbf{F}_C^{-1}\mathbf{C}^T$. Once $\{\tau\}$ and $\{\beta^p\}$ are solved, Eq. (36) can be expressed as

$$\{x_g\}=[\tilde{\mathbf{L}}^p]^T(\mathbf{F}^p-\mathbf{F}^p\mathbf{H}\mathbf{F}^p-\mathbf{F}^p\mathbf{K}_C\mathbf{F}_R-\mathbf{F}_R^T\mathbf{K}_C^T\mathbf{F}^p+\mathbf{F}_R)\tilde{\mathbf{L}}^p\{f_g\} \tag{45}$$

where

$$\mathbf{F}_R=\mathbf{R}^p([\mathbf{R}^p]^T\mathbf{K}_C\mathbf{R}^p)^{-1}[\mathbf{R}^p]^T,\ \mathbf{H}=\mathbf{K}_C-\mathbf{K}_C\mathbf{F}_R\mathbf{K}_C$$

In consequence, the global flexibility matrix can be expressed by the substructural flexibility matrix:

$$\mathbf{L}^p\mathbf{F}_g[\mathbf{L}^p]^T=\mathbf{F}^p-\mathbf{F}^p\mathbf{K}_C\mathbf{F}_R-\mathbf{F}_R\mathbf{K}_C\mathbf{F}^p-\mathbf{F}^p\mathbf{H}\mathbf{F}^p+\mathbf{F}_R \tag{46}$$

Based on Eq. (46), the substructural flexibility matrix $\mathbf{F}^p$ is extracted from the global flexibility $\mathbf{F}_g$ with an iterative scheme:

**1.** $\mathbf{F}^p$ is initiated from the diagonal subblocks of the global flexibility as

$$[\mathbf{F}^p]^{[0]}=\mathbf{L}^p\begin{bmatrix}\mathbf{F}_{\left(1:N^{(1)},1:N^{(1)}\right)} & & & \\ & \ddots & & \\ & & \mathbf{F}_{\left(\sum_{i=1}^{j-1}N^{(i)}+1:\sum_{i=1}^{j}N^{(i)},\sum_{i=1}^{j-1}N^{(i)}+1:\sum_{i=1}^{j}N^{(i)}\right)} & \\ & & & \ddots \\ & & & \mathbf{F}_{\left(\sum_{i=1}^{N_s-1}N^{(i)}+1:\sum_{i=1}^{N_s}N^{(i)},\sum_{i=1}^{N_s-1}N^{(i)}+1:\sum_{i=1}^{N_s}N^{(i)}\right)}\end{bmatrix}[\mathbf{L}^p]^T \tag{47}$$

**2.** In the $k$th ($k$ = 1, 2, …) iteration, the substructural flexibility matrix is calculated according to Eq. (46)

$$[\mathbf{F}^p]_0^{[k]} = \tilde{\mathbf{F}}_g + [\mathbf{F}^p]^{[k-1]}\mathbf{H}^{[k-1]}[\mathbf{F}^p]^{[k-1]} + [\mathbf{F}^p]^{[k-1]}\mathbf{K}_C^{[k-1]}\mathbf{F}_R^{[k-1]} + \mathbf{F}_R^{[k-1]}\mathbf{K}_C^{[k-1]}[\mathbf{F}^p]^{[k-1]} - \mathbf{F}_R^{[k-1]} \tag{48}$$

The diagonal subblocks of $[\mathbf{F}_0^p]^{[k]}$ are reused in the next iteration

$$[\mathbf{F}^p]^{[k]} = \begin{bmatrix} [\mathbf{F}^p]_0^{[k]}_{\left(1:N^{(1)},1:N^{(1)}\right)} & & & \\ & \ddots & & \\ & & [\mathbf{F}_0^p]_0^{[k]}_{\left(\sum_{i=1}^{j-1}N^{(i)}+1:\sum_{i=1}^{j}N^{(i)},\sum_{i=1}^{j-1}N^{(i)}+1:\sum_{i=1}^{j}N^{(i)}\right)} & \\ & & & \ddots \\ & & & [\mathbf{F}_0^p]_0^{[k]}_{\left(\sum_{i=1}^{N_s-1}N^{(i)}+1:\sum_{i=1}^{N_s}N^{(i)},\sum_{i=1}^{N_s-1}N^{(i)}+1:\sum_{i=1}^{N_s}N^{(i)}\right)} \end{bmatrix} \tag{49}$$

**3.** Step 2 stops when the substructural flexibility matrices from two consecutive iterations drop below a predefined tolerance [16]

$$e = \frac{norm\left([\mathbf{F}^p]^{[k]} - [\mathbf{F}^p]^{[k-1]}\right)}{norm\left([\mathbf{F}^p]^{[k]}\right)} \le Tol \tag{50}$$

The substructural flexibility matrices $\mathbf{F}^{(j)}$ are thereby gained by the diagonal subblocks of $[\mathbf{F}^p]^{[k]}$.

### 3.2. The projection matrix to extract free-free flexibility for model updating

In the substructuring methods, the global structure is divided properly into several independent free or constrained substructures. Most of the substructures are free-free without constraints after partition. Here the $j$th substructure is free-free as an illustration. The substructural flexibility matrix $\overline{\mathbf{F}}^{(j)}$ from $\mathbf{F}^p$ is constituted by both the rigid body modes and deformational modes. Hereinafter, superscript "$j$" is omitted to derive the free-free substructural flexibility for brevity. For the $j$th substructure, the substructural flexibility matrix, contributed by the rigid body motions and deformational motions, is expressed as

$$\overline{\mathbf{F}} = \mathbf{F} + \gamma \mathbf{R}\mathbf{R}^T \tag{51}$$

$\overline{\mathbf{F}}$ is defined as the generalized substructural flexibility. Accordingly, the generalized substructural stiffness matrix, including the contribution made by the rigid body motions and deformational motions is written as

$$\overline{\mathbf{K}} = \mathbf{K} + \eta \mathbf{R}\mathbf{R}^T \tag{52}$$

where $\overline{\mathbf{K}}$ is defined as the generalized substructural stiffness matrix. The free-free stiffness and flexibility matrices ($\mathbf{K}$ and $\mathbf{F}$) are contributed by the deformational modes solely. The participation factors $\gamma$ and $\eta$ of rigid body modes are difficult to determine, which makes the generalized flexibility unable to be applied to model updating or damage identification. It is necessary to extract the free-free substructural flexibility contributed by the deformational modes solely. The free-free flexibility shows the real properties of a substructure and can be applied to model updating and damage identification.

To remove the rigid body components in the generalized substructural stiffness, flexibility, and displacements, a projection matrix $\mathbf{P}$ is formed as [17]

$$\mathbf{P} = \mathbf{I} - \mathbf{R}(\mathbf{R}^T\mathbf{R})^{-1}\mathbf{R}^T \tag{53}$$

The projection matrix $\mathbf{P}$ has the properties of

$$\mathbf{P}^2 = \mathbf{P}, \mathbf{P}\mathbf{R} = \mathbf{R}^T\mathbf{P} = \mathbf{0} \tag{54}$$

$\mathbf{P}$ can filter out the rigid body motions, while the free-free stiffness and flexibility matrices contributed by the deformational modes remain unchanged

$$\begin{aligned} &\mathbf{F}\mathbf{P} = \mathbf{F}, \mathbf{P}\mathbf{F} = \mathbf{F}, \mathbf{P}\mathbf{F}\mathbf{P} = \mathbf{F} \\ &\overline{\mathbf{F}}\mathbf{P} = \mathbf{F}, \mathbf{P}\overline{\mathbf{F}} = \mathbf{F}, \mathbf{P}\overline{\mathbf{F}}\mathbf{P} = \mathbf{F} \\ &\mathbf{K}\mathbf{P} = \mathbf{K}, \mathbf{P}\mathbf{K} = \mathbf{K}, \mathbf{P}^T\mathbf{K}\mathbf{P} = \mathbf{K} \\ &\overline{\mathbf{K}}\mathbf{P} = \mathbf{K}, \mathbf{P}^T\overline{\mathbf{K}} = \mathbf{K}, \mathbf{P}^T\overline{\mathbf{K}}\mathbf{P} = \mathbf{K} \end{aligned} \tag{55}$$

On the other hand, the free-free stiffness and flexibility of a substructural analytical model are singular, whereas the generalized stiffness and flexibility are full-rank. The free-free stiffness and flexibility can be calculated from the inverse of the generalized stiffness and flexibility matrices as

$$\mathbf{F} = \mathbf{P}(\mathbf{K} + \eta \mathbf{R}\mathbf{R}^T)^{-1}\mathbf{P} \tag{56}$$

$$\mathbf{K} = \mathbf{P}(\mathbf{F} + \gamma \mathbf{R}\mathbf{R}^T)^{-1}\mathbf{P} \tag{57}$$

If the projection matrix $\mathbf{P}$ is known, the free-free substructural flexibility $\mathbf{F}$ is calculated from Eq. (56) or by removing all the rigid body components in the extracted substructural flexibility matrix (Eq. (55)). In substructure-based model updating, the elemental parameters of the analytical FE model are iteratively adjusted to minimize the discrepancy between the analytical substructural flexibility and that extracted from global data [18].

Generally, the stiffness or flexibility matrices are difficult to be measured on the full DOFs, and the partial stiffness and flexibility at the measured DOFs are probably utilized for a substructure. Divide the full-DOF model into the measured part and the unmeasured part, the stiffness matrix is rewritten in block form as

$$\mathbf{K} = \begin{bmatrix} \mathbf{K}_{aa} & \mathbf{K}_{ab} \\ \mathbf{K}_{ba} & \mathbf{K}_{bb} \end{bmatrix} \tag{58}$$

where subscript "*a*" represents the measured DOFs, and subscript "*b*" represents the unmeasured DOFs. The condensed stiffness matrix by the Guyan static condensation is [19–21]

$$\mathbf{K}_G = \mathbf{K}_{aa} - \mathbf{K}_{ab}\mathbf{K}_{bb}^{-1}\mathbf{K}_{ba} \tag{59}$$

The substructural flexibility is written in block form according to the measured and unmeasured parts as [22]

$$\mathbf{F} = \begin{bmatrix} \mathbf{F}_{aa} & \mathbf{F}_{ab} \\ \mathbf{F}_{ba} & \mathbf{F}_{bb} \end{bmatrix}, \overline{\mathbf{F}} = \begin{bmatrix} \overline{\mathbf{F}}_{aa} & \overline{\mathbf{F}}_{ab} \\ \overline{\mathbf{F}}_{ba} & \overline{\mathbf{F}}_{bb} \end{bmatrix} \tag{60}$$

In this case, the projection matrix of the reduced model $\mathbf{P}_D$ is formed as

$$\mathbf{P}_D = \mathbf{I} - \mathbf{R}_a(\mathbf{R}_a^T\mathbf{R}_a)^{-1}\mathbf{R}_a^T \tag{61}$$

which has the properties of

$$\mathbf{P}_D^2 = \mathbf{P}_D \tag{62}$$

$$\mathbf{P}_D\mathbf{R}_a = \mathbf{R}_a^T\mathbf{P}_D = \mathbf{0} \tag{63}$$

The rigid body modes $\mathbf{R}_a$ are gained by rewriting the rows in Eq. (58) corresponding to the measured DOFs.

The projection matrix $\mathbf{P}_D$ removes the rigid body components in the partial substructural flexibility matrix and leaves the free-free substructural flexibility by

$$\mathbf{F}_{aa}\mathbf{P}_D = \mathbf{P}_D\mathbf{F}_{aa} = \mathbf{P}_D\mathbf{F}_{aa}\mathbf{P}_D = \mathbf{F}_{aa} \tag{64}$$

$$\overline{\mathbf{F}}_{aa}\mathbf{P}_D = \mathbf{P}_D\overline{\mathbf{F}}_{aa} = \mathbf{P}_D\overline{\mathbf{F}}_{aa}\mathbf{P}_D = \mathbf{F}_{aa} \tag{65}$$

In addition, the projection matrix can be used to form the dual inverse of substructural stiffness and flexibility like

$$\mathbf{F}_{aa} = \mathbf{P}_D\left(\mathbf{K}_G + \mathbf{R}_a(\mathbf{R}_a^T\mathbf{R}_a)^{-1}\mathbf{R}_a^T\right)^{-1}\mathbf{P}_D \tag{66}$$

$$\mathbf{K}_G = \mathbf{P}_D\left(\mathbf{F}_{aa} + \mathbf{R}_a(\mathbf{R}_a^T\mathbf{R}_a)^{-1}\mathbf{R}_a^T\right)^{-1}\mathbf{P}_D \tag{67}$$

In substructure-based model updating, the elemental parameters in the substructural model are iteratively adjusted to minimize the discrepancy between the substructural flexibility and that extracted from global modal data [18]. For a free-free substructure, the flexibility extracted from global modal data is contaminated by the rigid body motions, and the stiffness matrix of substructural analytical FE model is singular. The projection matrix is utilized to extract the

free-free flexibility for model updating. On the one hand, the projection matrix removes the rigid body components in the generalized substructural flexibility from experimental data and leaves the free-free substructural flexibility according to

$$\mathbf{F}_{aa}^{E} = \mathbf{P}_D \overline{\mathbf{F}}_{aa}^{E} \mathbf{P}_D \tag{68}$$

On the other hand, the free-free flexibility matrix of the substructural FE model is iteratively computed from the singular stiffness matrix according to

$$\mathbf{F}_{aa}^{FE} = \mathbf{P}_D \left( \mathbf{K}_G + \mathbf{R}_a (\mathbf{R}_a^T \mathbf{R}_a)^{-1} \mathbf{R}_a^T \right)^{-1} \mathbf{P}_D \tag{69}$$

### 3.3. Substructure-based model updating

The substructure-based model updating process is listed in **Figure 2**. Identically, the *j*th substructure, which is free-free after partition, is employed to illustrate the substructure-based model updating in the following:

1. The experimental flexibility $\mathbf{F}_g^E$ is estimated by modal data of the global structure.

2. The generalized substructural flexibility matrix $\left(\overline{\mathbf{F}}^{(j)}\right)^E$ is extracted from the global flexibility matrix $\mathbf{F}_g^E$ by the proposed substructuring method in Section 3.1.

3. The rigid body modes $\mathbf{R}_a^{(j)}$ are constructed according to the nodal location of the *j*th substructure (Eq. (31)), and the projection matrix $\mathbf{P}^{(j)}$ is formed according to the proposed method in Section 3.2.

   The free-free substructural flexibility is extracted by the projection matrix as $\left(\mathbf{F}^{(j)}\right)^E = [\mathbf{P}^{(j)}]^T \left(\overline{\mathbf{F}}^{(j)}\right)^E \mathbf{P}^{(j)}$.

4. The FE model of the *j*th substructure is constructed without constraints. The FE model of the *j*th substructure is treated as an independent structure to be updated: In each iteration, the free-free substructural flexibility matrix $\left(\mathbf{F}^{(j)}\right)^{FE}$ at the measured DOFs and its sensitivity with respect to $\alpha$ $\partial\left(\mathbf{F}^{(j)}\right)^{FE}/\partial\alpha$ are computed [21]. The elemental parameters in the *j*th substructure are adjusted according to the sensitivity ($J(\alpha)$) of the flexibility with respect to elemental parameters, to minimize the objective function $\Delta\mathbf{F}(\alpha)$ through the Trust Region Newton method [2, 3, 18].

In the proposed substructuring method, the substructural flexibility matrices in primitive matrix $\mathbf{F}^p$ are independent. And only one substructure instead of the whole global structure at a time is updated in each iteration. The size of system matrices and updating parameters are sharply reduced, which improves the computational efficiency of model updating significantly.

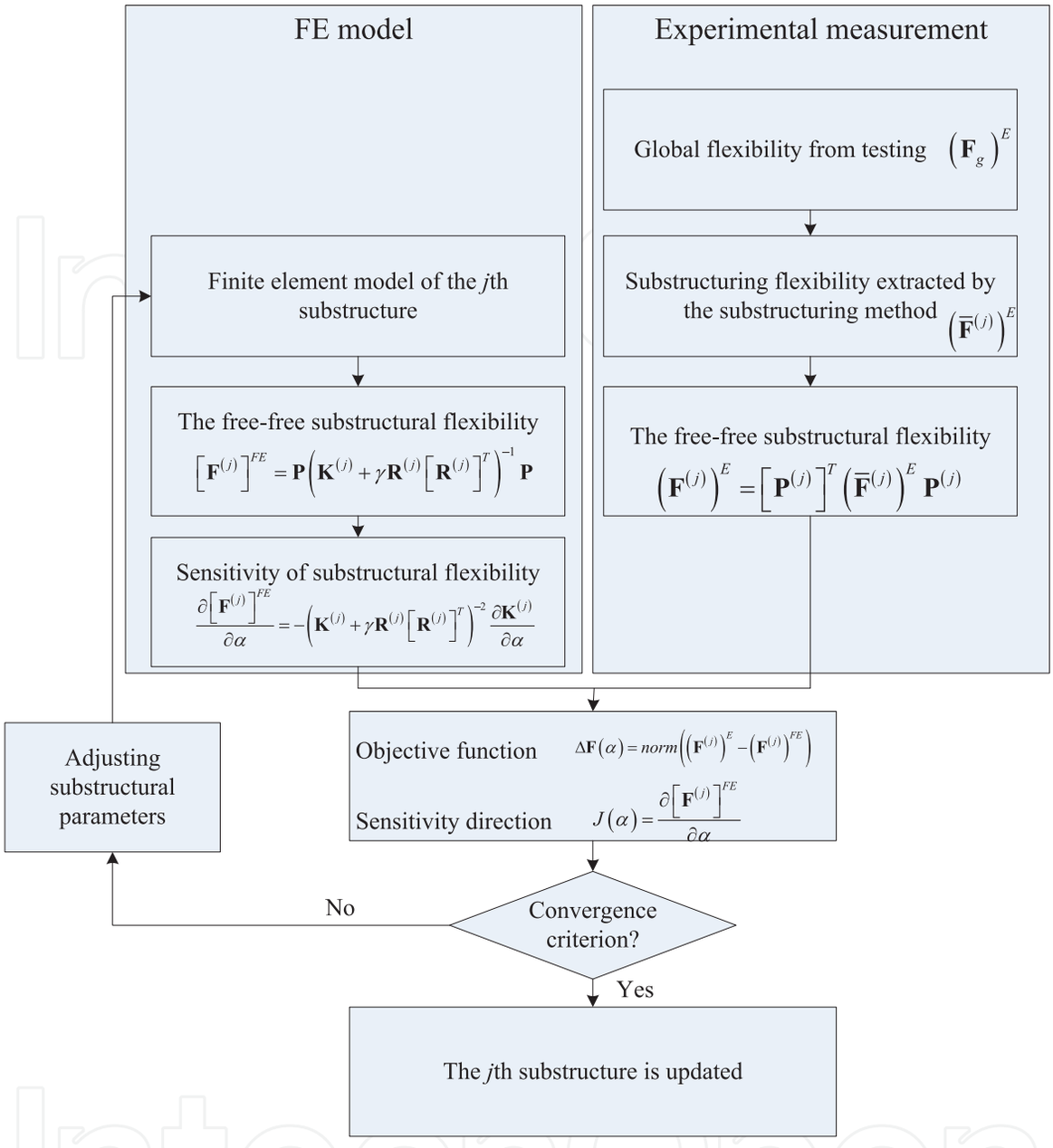


**Figure 2.** The model updating of inverse substructuring method.

## 4. Laboratory frame structure

Here a laboratory-tested steel frame structure is employed to investigate the effectiveness of the forward and inverse substructuring methods in model updating and damage identification. The cross section of the beams is 50.0 × 8.8 $mm^2$ and the cross section of the columns is 50.0 × 4.4 $mm^2$, with the dimensions shown in **Figures 3(a)** and **(b)**. The mass density of the structural material is 7.67 × $10^3$ $kg/m^3$. The FE model of the frame is composed of 44 nodes and 45 elements, with each element 100 mm in length as **Figure 3(c)**. In experiment, the accelerometers are placed at the nodes to measure the translational vibration of the frame [23]. The sampling

http://dx.doi.org/10.5772/67890

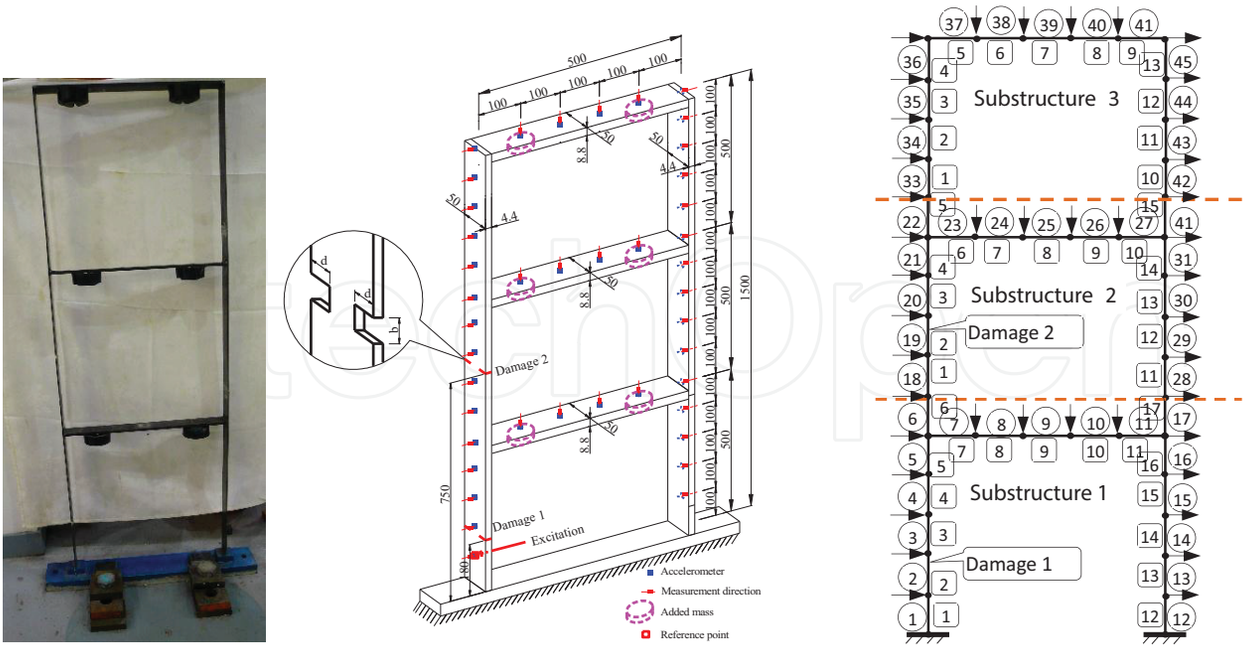


(a) Experimental specimen (b) Configurations (c) Analytical model

**Figure 3.** Laboratory-tested frame structure. (a) Experimental specimen. (b) Configurations. (c) Analytical model.

frequency was set to 2000 Hz. The specimen was excited with the instrumented hammer at the reference point indicated in **Figure 3(a)**.

The FE model is first updated in the undamaged state, and the refined model is subsequently used for damage identification. In the undamaged state, the Young's modules of all 45 elements are updated, with their initial values set to $2 \times 10^{11}$ Pa. The global structure is partitioned into three substructures, and the elements in the substructures are labeled in **Figure 3(c)**. Accordingly, there are 17 updating parameters in the first substructure, 15 in the second, and 13 in the third. The recorded input and output time history were analyzed in Matlab platform to derive the first 14 experimental frequencies and mode shapes.

Using the forward substructuring method, the first 30 modes in each substructure are selected as the master modes. In the model updating process, the substructure-based eigensolutions are compared with the first 14 experimental frequencies and mode shapes to form the objective function. The eigensensitivities are computed from one substructure solely to improve the computational efficiency. The elemental parameters of the FE model are adjusted iteratively to minimize the objective function through an optimal process. The elemental stiffness reduction factor (SRF) is used to estimate the damage identification, which gives the change ratio of the updated values to the initial values of updating parameters.

$$\mathrm{SRF} = \frac{\Delta\alpha}{\alpha} = \frac{\alpha^U - \alpha^O}{\alpha^O} \tag{70}$$

where superscript $O$ denotes the initial values before updating and $U$ denotes the updated values. The SRF values of the three substructures after updating are listed in **Figure 4(a)**. The model improved in the undamaged state is used for damage identification subsequently.

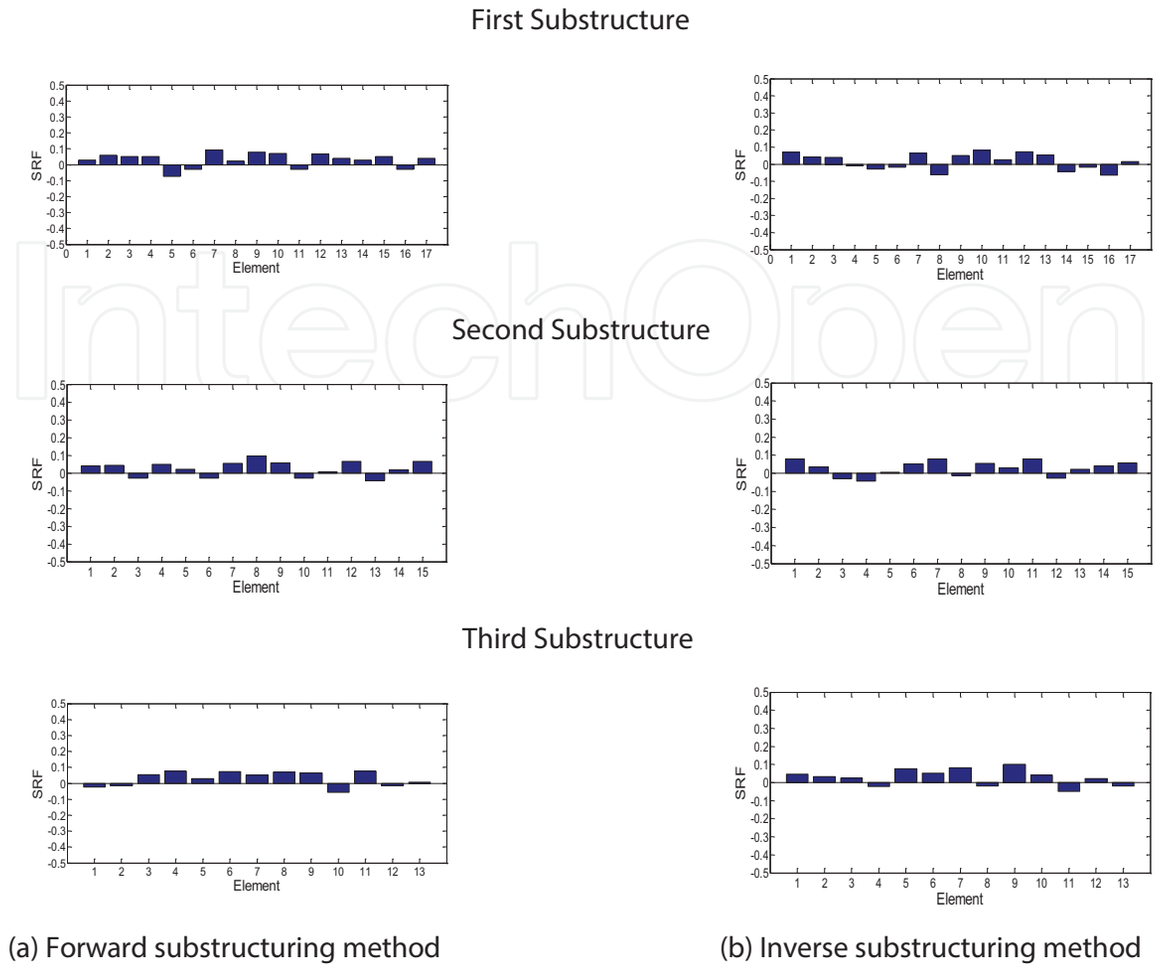


**Figure 4.** SRF values of the three substructures in the undamaged state. (a) Forward substructuring method. (b) Inverse substructuring method.

There are two damage configurations in the frame. In the first damage case, the column of the first storey is cut with the width of $b$ = 10 mm and depth $d$ = 15 mm at 180 mm away from the support (**Figure 3(b)**). Subsequently, the second storey is cut with the same width and depth at 750 mm away from the support.

In the first damage configuration, the cut is located in the first storey. The 17 elemental parameters in Substructure 1 are adjusted iteratively to minimize the discrepancy between the analytical eigensolutions and the measured modal data. In FE model updating, only the first substructure is reanalyzed, and the eigensolutions of the second and third substructures remain untouched and reused directly to compute the eigensolutions of global structure. The eigensensitivities with respect to the 17 elemental parameters are computed from the substructural derivative matrices of the first substructure solely, whereas those in the second and third substructures are zero-matrices. The elemental parameters in the undamaged state are subsequently employed for damage identification. It is apparent from **Figure 5(a)** that, Element 2 has an obvious negative value in SRF of about −25%, which agrees with the location of the cut in the experiment.

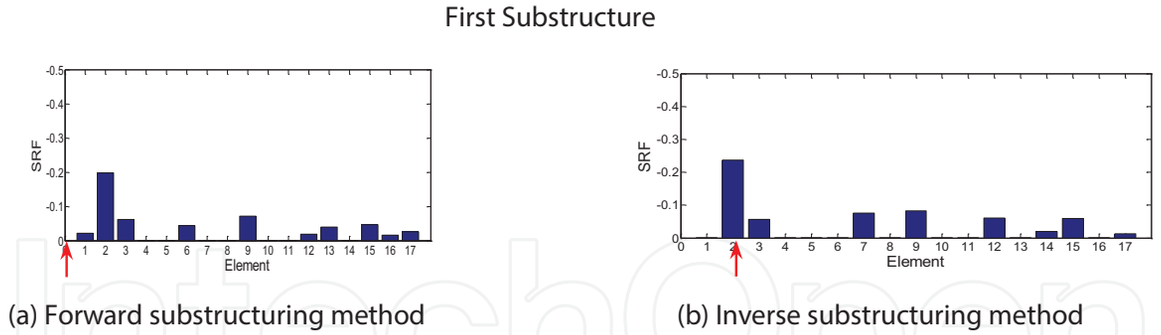


**Figure 5.** SRF values of the first damage configuration. (a) Forward substructuring method. (b) Inverse substructuring method. ↑ Actual damage location.

In the second damage configuration, the two cuts are located in the first and second substructures, respectively. Subsequently, the first and second substructures are updated, while the third substructure remains untouched. The SRF values shown in **Figure 6(a)** demonstrate that Element 2 of the first substructure and Element 2 of the second substructure have an obvious negative SRF values. The identified locations agree with those of the experimental cut. Particularly, the SRF values of Element 2 of the first substructure are about −23%, comparable to that in the first damage configuration. This is because the cut remains unchanged in the two damage configurations.

Afterwards, the frame structure is analyzed by the inverse substructuring method with the same measured data and FE model. In the undamaged state, the global flexibility is formulated from the 14 pairs of measured natural frequencies and mode shapes. The inverse substructuring method is used to extract the substructural flexibility matrices of the three

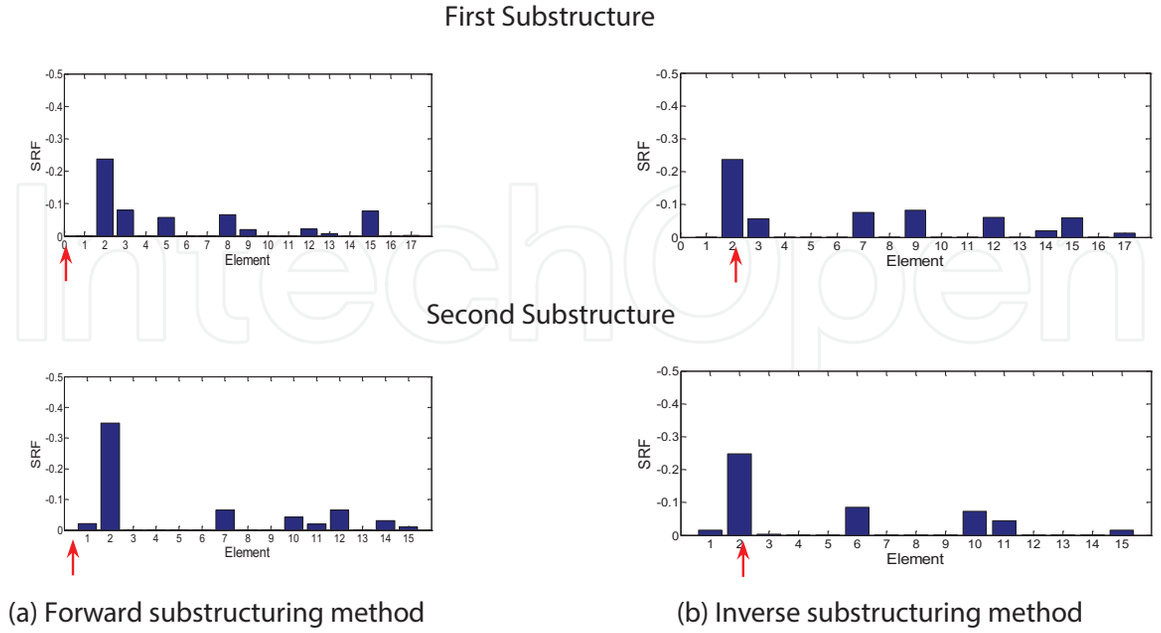


**Figure 6.** SRF values of the second damage configuration. (a) Forward substructuring method. (b) Inverse substructuring method. ↑ Actual damage location.

substructures simultaneously. The global FE model is divided into three substructures as well. The substructural flexibility of the three submodels is compared with the extracted substructural flexibility to form the objective function. The discrepancy of substructural flexibility matrices between the FE sub-model and extracted ones is minimized by adjusting the updating elemental parameters of the three submodels independently. **Figure 4(b)** reports the updated SRF values of the three substructures, which are subsequently utilized for damage identification.

In the first damage case, the local area within the first storey, i.e., Nodes 1 to 18 in **Figure 3(c)**, are measured. Accordingly, only the substructural flexibility matrix of the first storey is extracted, based on which the submodel of the first substructure is updated independently. **Figure 5(b)** reveals a significant reduction in stiffness in Element 2, which agrees with the real location of the cut in experiment. The identified damage location and severity agrees with those obtained by the forward substructuring method as well.

In the second damage configuration, the frequencies and mode shapes measured in the first and second storeys are measured to form the global flexibility matrix. The substructural flexibility corresponding to the first and second substructures are extracted from the global flexibility simultaneously. The submodels of the first and second substructures are independently updated to recover the extracted substructural flexibility. **Figure 6(b)** reveals a negative SRF value of −20% in Element 2 of the first substructure and −25% in Element 2 of the second substructure. The identified damage location and severity are consistent to those gained by the forward substructuring method again. Both the forward and inverse substructuring methods are effective in model updating and damage identification.

## 5. Conclusion

A forward substructuring method and an inverse substructuring method are proposed in this chapter for model updating and damage identification. In the forward substructure-based model updating, the modified substructures are reanalyzed and assembled with other untouched substructures for the eigensolutions of the global structure to match the experimental data in an optimal manner. In the inverse substructuring method, the experimental modal data measured in local areas are used to extract the experimental flexibility matrix of the concerned substructure. The concerned substructures are updated by being treated as independent structures. Both the forward and inverse substructuring methods are effective in model updating and damage identification of a laboratory-tested steel frame structure. In the substructure-based model updating, only one substructure instead of the large-scale global structure is re-analyzed, which will be quite efficient for the model updating of practical large-scale structures. The substructuring methods are promising to be combined with the nonlinear analysis, vibration control, and parallel computation as well.

## Author details

Shun Weng[1]*, Hong-Ping Zhu[1], Yong Xia[2] and Fei Gao[1]

*Address all correspondence to: wengshun@mail.hust.edu.cn

1 School of Civil Engineering and Mechanics, Huazhong University of Science and Technology, Wuhan, Hubei, P. R. China

2 Department of Civil and Structural Engineering, The Hong Kong Polytechnic University, Hung Hom, Kowloon, Hong Kong

## References

[1] Mottershead JE, Friswell MI. Model updating in structural dynamics: a survey. Journal of Sound and Vibration. 1993;**167**:347–375. DOI: 10.1006/jsvi.1993.1340

[2] Bakira PG, Reynders E, Roeck GD. Sensitivity-based finite element model updating using constrained optimization with a trust region algorithm. Journal of Sound and Vibration. 2007;**305**: 211–225. DOI: 10.1016/j.jsv.2007.03.044

[3] Mottershead JE, Link M, Friswell MI. The sensitivity method in finite element model updating: a tutorial. Mechanical Systems and Signal Processing. 2011;**25**:2275–2296. DOI: 10.1016/j.ymssp.2010.10.012

[4] Klerk D, Rixen DJ, Voormeeren SN. General framework for dynamic substructuring: history, review, and classification of techniques. AIAA Journal. 2008;**46**:1169–1181. DOI: 10.2514/1.33274

[5] Weng S, Xia Y, Xu YL, Zhou XQ, Zhu HP. Improved substructuring method for eigensolutions of large-scale structures. Journal of Sound and Vibration. 2009;**323**:718–736. DOI: 10.1016/j.jsv.2009.01.015

[6] Weng S, Zhu HP, Xia Y, Mao L. Damage detection using the eigenparameter decomposition of substructural flexibility matrix. Mechanical Systems and Signal Processing. 2013;**34**:19–38. DOI: 10.1016/j.ymssp.2012.08.001

[7] Weng S, Xia Y, Xu YL, Zhu HP. Substructure based approach to finite element model updating. Computers and Structures. 2011;**89**:772–782. DOI: 10.1016/j.compstruc.2011.02.004

[8] Choi D, Kim H, Cho M. Iterative method for dynamic condensation combined with substructuring scheme. Journal of Sound and Vibration. 2008;**317**:199–218. DOI: 10.1016/j.jsv.2008.02.046

[9] Weng S, Zhu HP, Xia Y, Zhou XQ, Mao L. Substructuring approach to the calculation of higher-order eigensensitivity. Computers and Structures. 2013;**117**:23–33. DOI: 10.1016/j.compstruc.2012.11.005

[10] Bathe KJ, Wilson EL. Numerical Methods in Finite Element Analysis. Prentice-Hall Inc. Englewood chiffs, New Jersey: Wiley; 1989. DOI: 10.1002/nag.1610010308

[11] Sehmi NS. Large order structural eigenanalysis techniques algorithms for finite element systems. England, Ellis Horwood Limited, Chichester: Wiley; 1989. DOI: 10.1002/cnm.1630060609

[12] Fox RL, Kapoor MP. Rate of change of eigenvalues and eigenvectors. AIAA Journal. 1968;**6**:2426–2429.

[13] Nelson RB. Simplified calculation of eigenvector derivatives. AIAA Journal 1976;**14**:1201–1205.

[14] Perera R, Ruiz A. A multistage FE updating procedure for damage identification in large-scale structures based on multiobjective evolutionary optimization. Mechanical Systems and Signal Processing. 2008;**22**:970–991. DOI: 10.1016/j.ymssp.2007.10.004

[15] Ewins DJ. Modal Testing: Theory, Practice and Application. 2th ed. Baldock, England: Research Studies Press; 2000.

[16] Alvin KF, Park KC. Extraction of substructural flexibility from global frequencies and mode shapes. AIAA Journal. 1999;**37**:1444–1451. DOI: 10.2514/2.621

[17] Doebling SW, Peterson LD. Experimental determination of local structural stiffness by disassembly of measured flexibility matrices. Journal of Vibration and Acoustics. 1998; **120**:949–957. DOI: 10.1115/1.2893925

[18] Felippa CA, Park KC, Filho MRJ. The construction of free-free flexibility matrices as generalized stiffness inverses. Computers & Structures. 1998;**68**:411–408. DOI: 10.1016/S0045-7949(98)00068-6

[19] Jaishi B, Ren WX. Damage detection by finite element model updating using modal flexibility residual. Journal of Sound and Vibration. 2006;**290**:369–387. DOI: 10.1016/j.jsv.2005.04.006

[20] Guyan RJ. Reduction of stiffness and mass matrices. AIAA Journal. 1965;**3**:380. DOI:10.2514/3.2874

[21] Xia Y, Lin RM. Improvement on the iterated IRS method for structural eigensolutions. Journal of Sound and Vibration. 2004;**270**:713–727. DOI: 10.1016/S0022-460X(03)00188-3

[22] Xia Y, Lin RM. A new iterative order reduction (IOR) method for eigensolutions of large structures. International Journal for Numerical Method in Engineering. 2004;**59**:153–172. DOI: 10.1002/nme.876

[23] Formenti DL, Richardson MH. Parameter estimation from frequency response measurements using rational fraction polynomials. In: The 20th International Modal Analysis Conference; 04–07 February 2002; Los Angeles, CA; 2002. pp. 1–10.